Please cite this article in press as: Rang et al., Temporal Dynamics of Bacterial Aging and Rejuvenation, Current Biology (2011), doi:10.1016/j.cub.2011.09.018

Current Biology *21*, 1–4, November 8, 2011 ©2011 Elsevier Ltd All rights reserved DOI 10.1016/j.cub.2011.09.018

Report

Temporal Dynamics of Bacterial Aging and Rejuvenation

Camilla U. Rang,[1,2] Annie Y. Peng,[1,2] and Lin Chao[1,2,*]
[1]Section of Ecology, Behavior and Evolution, Division of Biological Sciences, University of California, San Diego, La Jolla, CA 92093-0116, USA

Summary

Single-celled organisms dividing by binary fission were thought not to age [1–4]. A 2005 study by Stewart et al. [5] reversed the dogma by demonstrating that *Escherichia coli* were susceptible to aging. A follow-up study by Wang et al. [6] countered those results by demonstrating that *E. coli* cells trapped in microfluidic devices are able to sustain robust growth without aging. The present study reanalyzed these conflicting data by applying a population genetic model for aging in bacteria [7]. Our reanalysis showed that in *E. coli*, as predicted by the model, (1) aging and rejuvenation occurred simultaneously in a population; (2) lineages receiving sequentially the maternal old pole converged to a stable attractor state; (3) lineages receiving sequentially the maternal new pole converged to an equivalent but separate attractor state; (4) cells at the old pole attractor had a longer doubling time than ones at the new pole attractor; and (5) the robust growth state identified by Wang et al. corresponds to our predicted attractor for lineages harboring the maternal old pole. Thus, the previous data, rather than opposing each other, together provide strong evidence for bacterial aging.

Results and Discussion

The population genetic model used for our study was originally constructed to provide a predictive framework for studying the evolution of bacterial aging [7]. Because bacterial aging was attributed to the accumulation of nongenetic (e.g., oxidative) damage in aging cells [8], the model was designed to describe the partitioning of such damage by a mother bacterium to her daughters. The model revealed that a mother that partitions asymmetrically more damage to one daughter has a higher evolutionary fitness. Asymmetry is advantageous because it creates fitness variance for natural selection. The daughter receiving less damage is rejuvenated and the one receiving more ages.

The model also tracked the partitioning of damage in relation to the two poles of a bacterial cell. *E. coli* cells divide by cleaving their long axis with a division plate. Because two new poles are formed at the plate, poles distal to the plate are the old poles and every bacterium has a new and an old pole. Whenever a mother bacterium divides, one daughter receives the maternal old pole and the other receives the maternal new pole. The model found that if bacterial lineages receiving sequentially the maternal old pole were tracked, their doubling times converged onto a stable attractor state. The doubling times of lineages receiving likewise the maternal new pole converged onto an equivalent but different attractor state. More importantly, the bacteria at the old pole attractor were more aged and had a longer doubling time. If bacteria were symmetrical, old and new poles would converge to a single attractor and aging would not be evident. Thus, bacterial aging evolves because natural selection favors bacteria that partition damage asymmetrically.

The attractor states and temporal dynamics of bacterial aging and rejuvenation predicted by the model can be visualized graphically on a phase plane onto which the doubling times of daughter cells harboring the new and maternal old poles (T_1 and T_2, respectively) are graphed against the doubling time of their mother cell (T_0) (Figure 1). Hereafter, daughters 1 and 2, or simply new and old pole cells, will be used as notations for the daughters harboring the new and maternal old poles. Besides demonstrating the old and new pole attractors, the phase plane also shows that not all cells reside at the two attractors. For example, if a mother cell resides at the old pole attractor, its daughter 2 is expected to have the doubling time of the attractor, but its daughter 1 will be far away from the new pole attractor. The lineage descending from this daughter 1, as all other new pole lineages, should then converge to the new pole attractor.

By fitting the data of Stewart et al. [5] to our model, we had previously confirmed the locations of the predicted T_1 and T_2 attractors [7]. However, those results were based solely on a static snapshot of bacterial doubling times on a phase plane. To test the model more completely and rigorously, it would be desirable to determine whether the additional temporal dynamics predicted by the model are realized. To achieve such a goal, we used our model to make new and explicit predictions and tested them against novel data extracted from previously published data.

From the results of Stewart et al., we first generated data to test the prediction that the new and old pole lineages should converge over time to two attractors. In our previous static analysis of their data, we had examined only the doubling times of 128 mother cells and their 256 daughters over two generations [7]. However, the data go back eight generations to the origin of the population from a single mother cell. Thus, longer and continuous temporal dynamics of a lineage could be extracted. Such lineage dynamics were obtained by recovering the doubling time of all new poles of the lineage descending from the original cell (see Supplemental Information available online), or what is termed an *nnnnnnnn* lineage over eight generations. Likewise, data for an old pole or *oooooooo* lineage were also extracted. For comparison, *ooonnnnn* and *nnnooooo* lineages, which harbored for the three initial generations the alternate pole, were also obtained. The results remarkably confirmed the temporal dynamics predicted by the model (Figure 2). In each case, the lineages converged to the appropriate attractors, whose positions had been estimated in our previous study [7]. In the lineages that were switched after three generations, the tracking responded accordingly after the change. Because the lineages tracked from right to left, the ones converging onto the new pole attractor did not have sufficient time to encircle the

[2]These authors contributed equally to this work
*Correspondence: lchao@ucsd.edu

Please cite this article in press as: Rang et al., Temporal Dynamics of Bacterial Aging and Rejuvenation, Current Biology (2011), doi:10.1016/j.cub.2011.09.018

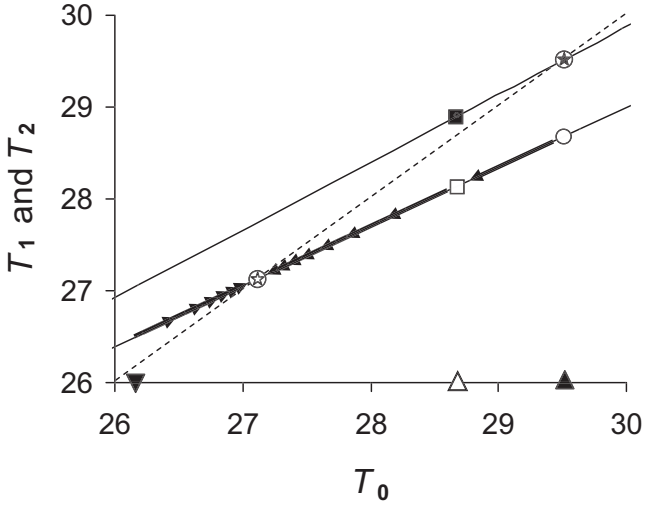

Figure 1. Graphical Prediction for Aging and Rejuvenation in Bacteria

Unless otherwise specified, black and white symbols refer respectively to old and new poles in this and subsequent figures. Predictions based on model of Chao [7] and are presented on a phase plot of T_1 and T_2 as a function of T_0. T_1 and T_2 are the doubling times of daughters 1 and 2, which receive the new and old poles, respectively, of the mother cell. T_0 is the doubling time of the mother cell. The predicted relationships are represented as two solid lines (lower, T_1; upper, T_2). The dashed line is the identity line. The intercept of the identity line and the T_1 and T_2 graph lines corresponds to attractor states to which the new and old pole lineages converge (☆, ★). To illustrate the convergence, consider a mother cell with a doubling time of 29.5 min. Projecting upwards from T_0 = 29.5 (▲) to the two solid lines identifies the two points ○ and ★, which are the predicted T_1 and T_2 values for the mother cell's two daughters. In preparation for a later discussion, we denote ○ as $\tilde{T}_1$. Following only the new pole lineage, let the $\tilde{T}_1$ become a mother by projecting its doubling time onto the T_0 axis (△). $\tilde{T}_1$'s daughters will have the doubling times T' and T'' (□, ■). By tracking $\tilde{T}_1$ and T', the new pole lineage progresses downwards along the T_1 graph line (rightmost arrow). Because $\tilde{T}_1$ is greater than T', the progression corresponds to rejuvenation. If the T' daughter and its subsequent daughters are likewise projected in turn onto the T_0 axis as mothers, the resulting new pole lineage converges to the lower attractor (☆). If the initial mother cell had a T_0 = 26.2 min (▼), a similar convergence occurs, albeit from the left of the attractor (leftmost arrows), and the increase in doubling times corresponds to aging. Note that the old pole graph line also has its own attractor point (★). These attractors are stable equilibrium points and are hereafter denoted $\hat{T}_1$ and $\hat{T}_2$, respectively. A bacterial population consists of a dynamical network of cells connected by cell division. Some cells reside at the attractor states, but others emanate from them and their lineages and converge to the alternate attractor. Note that the points in this figure illustrate qualitatively that the relationships $\hat{T}_2 > T'' > \tilde{T}_1 > T'$ and $[\hat{T}_2 - T''] > [\tilde{T}_1 - T']$, which will be used in Figure 3 for data testing.

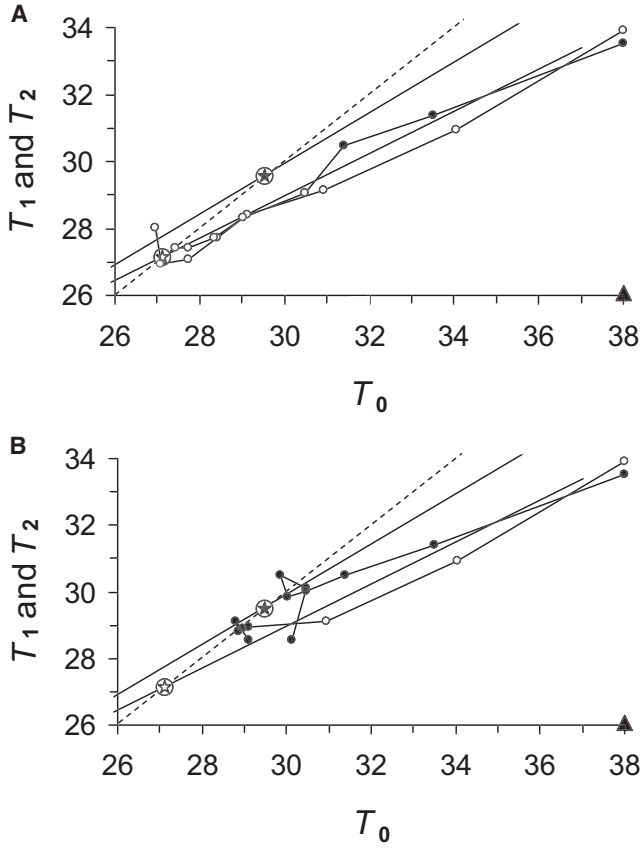

Figure 2. Observed Temporal Dynamics of Aging and Rejuvenation Tracked in Lineages of *E. coli* Descending from a Single Mother Cell

For interpretation of the plot and definitions, see Figure 1. These results provide the experimental complement of the projection described in Figure 1 for a new pole lineage. Data were extracted from Stewart et al. [5]. All lineages descended from a single mother cell that had a doubling time of 38 min (▲) and were tracked for eight generations. ★ is the attractor for old pole lineages or $\hat{T}_2$; ☆ is the attractor for new pole lineages or $\hat{T}_1$. The positions of the attractors at 29.5 and 27.2 min are predicted by our previous analysis [7] of the data of Stewart et al.

(A) Lineage *nnnnnnnn* (—○—○—) was tracked by following only the doubling times of cells receiving the new pole from a mother. Lineage *ooonnnnn* (—●—○—) was tracked for three generations by old pole cells and then crossed over to new poles.

(B) Lineages *oooooooo* (—●—●—); *nnnooooo* (—○ —●—) were tracked by reversing the order of new and old poles in (A).

attractor (Figure 2A). The old pole lineages clearly show dynamics encircling the corresponding attractor (Figure 2B). However, the trajectories around the old pole attractor were not well superimposed, which suggests that there is stochasticity and error to the process.

The data from Wang et al. [6] provided the second test. As indicated above, these data reported stable and robust growth of trapped *E. coli* cells over hundreds of generations and were interpreted to be at odds with bacterial aging. However, our conjecture was that the robust state was simply the confirmation of the old pole attractor predicted by our model. Because any new pole remains a new pole for only one generation, all trapped cells harbor an old pole after one generation and eventually should converge onto the old pole attractor. We tested our conjecture by extracting new data from Wang et al.'s study and determining whether the doubling time of cells descending from their robust state matched values predicted by our model for cells emanating from an old pole attractor (Supplemental Information). Because the depth of the channels in Wang et al.'s microfluidic device retained cells for only three generations, the predictions were limited to that time horizon. Four types of cells were tracked. The cells and their doubling times were denoted $\tilde{T}_1$, $\hat{T}_2$, T', and T'', where $\tilde{T}_1$ and $\hat{T}_2$ were respectively daughters 1 and 2 of a cell at the old pole attractor and T' and T'' were respectively daughters 1 and 2 of a $\tilde{T}_1$ cell. Two explicit predictions were made: (1) the doubling times should have the ranking $\hat{T}_2 > T'' > \tilde{T}_1 > T'$, and (2) the difference $[\hat{T}_2 - T'']$ should be greater than $[\tilde{T}_1 - T']$. Figure 1 provides a graphical interpretation of the four cell types and the meaning of the rankings. Analytical proofs for the rankings are available as Supplemental Information. Data extracted from Wang et al. fully confirmed the two predictions (Figure 3).

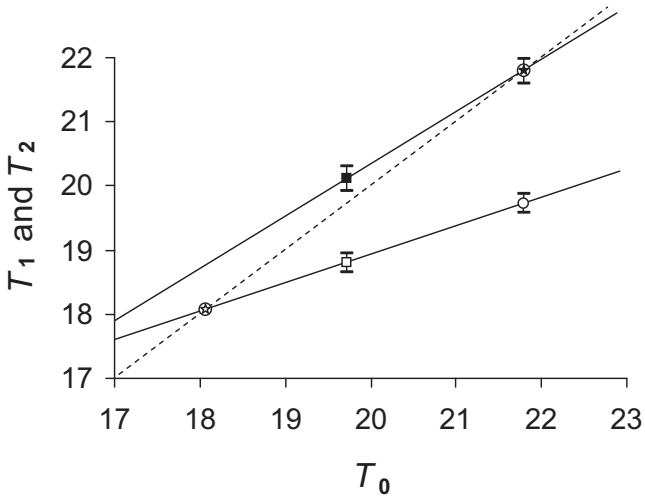

Figure 3. Observed Temporal Dynamics of Aging and Rejuvenation Emanating from Wang et al.'s Robust Stable State

For definitions, color code, and interpretation of the dynamics of the phase plot see Figure 1. The four points (✪, ○, □, and ■) represent observed estimates of $\hat{T}_2$, $\tilde{T}_1$, T', and T'', which are as defined in Figure 1 and correspond to the old pole or $\hat{T}_2$ attractor and the daughter cells descending from it. Estimates were extracted from the data of Wang et al. [6] by assuming that the robust state was the old pole attractor. Estimated averages for $\hat{T}_2$, T'', $\tilde{T}_1$, and T' had values of 21.8, 20.1, 19.7, and 18.8 min. These averages and their plot confirm the prediction that $\hat{T}_2 > T'' > \tilde{T}_1 > T'$. All averages were significantly different from each other. Error bars correspond to 95% confidence limits (n = 618), which never overlapped. Estimates from the data also supported the prediction that $[\hat{T}_2 - T''] > [\tilde{T}_1 - T']$. We estimated that $[\hat{T}_2 - T''] = 1.68$ and $[\tilde{T}_1 - T'] = 0.92$ and found these average values to be significantly different (standard error of the mean = 0.101 and 0.136; n = 618; $p < 0.0000005$). The confirmation of the predictions shows that Wang et al.'s robust attractor is equivalent to the old pole attractor of our model. Solid lines are drawn through the four points to represent the possible relationship corresponding to our model. Extending the lower solid line to its intersection with the dashed identity line predicts that the unrecorded $\hat{T}_1$ value in Wang et al.'s system is approximately 18 min (✪).

Data values matched to our model yielded doubling times that ranked $\hat{T}_2 > T'' > \tilde{T}_1 > T'$ as 21.8 > 20.1 > 19.7 > 18.8 min. The ranking $[\hat{T}_2 - T''] > [\tilde{T}_1 - T']$ was estimated as1.68 > 0.92 min. All predictions were found to be significantly different on the basis of nonoverlapping 95% confidence limits (Figure 3).

The rankings we tested are more than simple numerical relationships. They reflect fundamental temporal changes predicted by the model. The fact that $\hat{T}_2$ was greater than T'', $\tilde{T}_1$, and T' shows that Wang et al.'s robust state was likely the old pole attractor and that there was a second attractor at which the doubling times would be shorter. The $\tilde{T}_1$ cells were the first step away from Wang et al.'s robust state. Although old pole cells at the robust state do not age, new cycles of both aging and rejuvenation are triggered by $\tilde{T}_1$ cells and their T'' and T' daughters. The fact that $\tilde{T}_1$ and T' were the shortest doubling times demonstrates rejuvenation resulting from the allocation of less damage. The fact that $\tilde{T}_1 > T'$ shows that not only does $\tilde{T}_1$ escape the robust state, its daughter moves even farther away, presumably toward our second and predicted attractor for the new pole. The fact that T'' is the second longest doubling time shows that it, as an old pole, is beginning to converge back to the old pole attractor. Altogether, these results provide strong support that Wang et al.'s robust state is our old pole attractor. Additionally, the relationship $T'' > \tilde{T}_1$ is significant because it shows that the slope of T_2 as a function of T_0 (the T_2 graph line in Figure 1) is less than one. A slope of less than one is needed for the function to intercept the identity line and generate the old pole attractor (Figure 1). The slope equals $[\hat{T}_2 - T'']/[\hat{T}_2 - \tilde{T}_1]$ and is less than one if $[\hat{T}_2 - \tilde{T}_1] > [\hat{T}_2 - T'']$, which is true when $T'' > \tilde{T}_1$. Finally, the second prediction that $[\hat{T}_2 - T''] > [\tilde{T}_1 - T']$ results from the fact that the slope of the T_2 graph line should be greater than that of T_1 (Figure 1). If it is greater, then the T_1 graph line has a slope that is less than one and thus also intercepts the identity line to create the new pole attractor. Although the data of Wang et al. do not provide a measurement of the new pole attractor, our analysis predicts that it should have a value of approximately 18 min (see Figure 3). It is noteworthy that the different slopes of the T_1 and T_2 lines result because the mapping relationship between damage and doubling time in our model is not linear. This nonlinearity was not intentionally assumed or built into the model (see Supplemental Information). The manifestation of this nonlinearity in Wang et al.'s data shows that an emergent property of the model is confirmed in bacteria.

We have reconciled the opposing results of Stewart et al. and Wang et al. by reanalyzing their data from the perspective of a population genetic model. The model predicts that old pole and new pole lineages should converge to two separate attractor states and that the convergences follow distinctive trajectories. Our analysis of the model and its predictions reveals previously unknown temporal dynamics of bacterial aging. They also resolve the origin of Wang et al.'s robust state by showing that it corresponds to the old pole attractor. The notion that natural selection could favor aging or loss of function can appear paradoxical, if function were to equal fitness [2]. Our model shows that asymmetry, while introducing aging, elevates the lifetime fitness [7]. The existence of aging in bacteria suggests that the phenomenon could have evolved with the first single-celled organism and for the same reason in both prokaryotes and eukaryotes. Bacterial data on aging detail the process over hundreds of generations and may provide the case in which the evolution of aging is first and best understood. Although aging in bacteria and aging in eukaryotes may appear distinct, the difference is minimized if bacteria carrying the old pole, and receiving more damage, are regarded as mother cells. On the other hand, if aging in eukaryotes evolved for a different reason, bacterial aging may then provide the exception that proves the difference.

Supplemental Information

Supplemental Information includes Supplemental Experimental Procedures and can be found with this article online at doi:10.1016/j.cub.2011.09.018.

Acknowledgments

We thank Ellsworth Campbell, David Nguyen, Terry Hwa, Minsu Kim, and Alex Groisman for discussion and assistance during the completion of this study.

Received: June 9, 2011
Revised: August 25, 2011
Accepted: September 9, 2011
Published online: October 27, 2011

References

1. Partridge, L., and Barton, N.H. (1993). Optimality, mutation and the evolution of ageing. Nature *362*, 305–311.
2. Rose, M.R. (1991). Evolutionary Biology of Aging (Oxford: Oxford University Press).

Please cite this article in press as: Rang et al., Temporal Dynamics of Bacterial Aging and Rejuvenation, Current Biology (2011), doi:10.1016/j.cub.2011.09.018

3. Turke, P.W. (2008). Williams's theory of the evolution of senescence: still useful at fifty. Q. Rev. Biol. *83*, 243–256.
4. Williams, G.C. (1957). Pleiotropy, natural selection, and the evolution of senescence. Evolution *11*, 398–411.
5. Stewart, E.J., Madden, R., Paul, G., and Taddei, F. (2005). Aging and death in an organism that reproduces by morphologically symmetric division. PLoS Biol. *3*, e45.
6. Wang, P., Robert, L., Pelletier, J., Dang, W.L., Taddei, F., Wright, A., and Jun, S. (2010). Robust growth of Escherichia coli. Curr. Biol. *20*, 1099–1103.
7. Chao, L. (2010). A model for damage load and its implications for the evolution of bacterial aging. PLoS Genet. *6*, e1001076.
8. Lindner, A.B., Madden, R., Demarez, A., Stewart, E.J., and Taddei, F. (2008). Asymmetric segregation of protein aggregates is associated with cellular aging and rejuvenation. Proc. Natl. Acad. Sci. USA *105*, 3076–3081.